A forced Korteweg-de Vries model for nonlinear mixing of oscillations in a dusty plasma

Ajaz A. Mir,[1] Sanat K. Tiwari,[1,*] John Goree,[2] Abhijit Sen,[3] Chris Crabtree,[4] and Gurudas Ganguli[4]

[1] *Indian Institute of Technology Jammu, Jammu, J&K, 181221, India*
[2] *Department of Physics and Astronomy, University of Iowa, Iowa City, IA 52242, USA*
[3] *Institute for Plasma Research, Gandhinagar, Gujarat, 382428, India*
[4] *Naval Research Laboratory, Washington, DC 20375, USA*

(Dated: September 18, 2020)

Nonlinear mixing of oscillations in a dusty plasma due to the harmonic time varying modulation of a nonlinear compressional oscillation is analyzed using a simple mathematical model consisting of a forced Korteweg-de Vries equation. An exact analytic solution of this equation is found to exhibit nonlinear mixing in the system. The model solution can be usefully employed to predict the existence of nonlinear mixing of oscillations in a two-dimensional dusty plasma system of a particular experimental configuration.

I. INTRODUCTION

Nonlinear mixing is a phenomenon found in many physical systems that can sustain waves of large amplitudes [1–4]. In a dusty plasma, compressional waves can easily attain large amplitudes, even if the electric potential variation is only a few millivolts, and this is due to the large electric charge of thousands of elementary charges [4, 5] residing on a dust particle.

Two kinds of compressional waves in dusty plasmas are the dust-acoustic wave and the longitudinal dust lattice wave [6–8]. The dust-acoustic wave (DAW) propagates in a three-dimensional cloud of charged dust particles which are immersed in a mixture of electrons and ions; all three of these charged species participate in the compression and rarefaction. If there is an ambient steady electric field, it will drive an ion current that can easily self-excite the DAW through an instability, which commonly occurs in laboratory gas-discharge plasmas [9, 10]. On the other hand, the longitudinal dust lattice wave (DLW) propagates in a different situation; while the electrons and ions fill a three-dimensional volume, the dust particles do not; they are instead confined to a planar layer which is thin, and often is just a monolayer. Because of the paucity of dust particles, the electrons and ions are not significantly affected by the dust particles, and for the most part they just contribute to the Debye screening of the inter-particle repulsion among the dust particles [6]. Unlike the DAW, the longitudinal dust lattice wave is not necessarily excited by an ambient DC electric field, so that in the laboratory it is common to excite it by an external forcing [11, 12].

In this paper we consider the longitudinal dust lattice wave, with two sinusoidal external excitations at a large amplitude, to cause nonlinear mixing. By perturbing a two-dimensional crystalline layer of dust particles using two laser beams of different frequencies, three-wave mixing was experimentally demonstrated by Nosenko *et al.* [13]. In this paper, we theoretically demonstrate nonlinear mixing phenomenon in a dusty plasma system using an analytic solution of a sinusoidally forced Korteweg-de Vries model equation. The model solution can also be usefully employed to predict the existence of nonlinear mixing in a variant of the two-dimensional experimental dusty plasma experiment reported in Ref. [13].

In their experiment, the authors of Ref. [13] used a horizontal monolayer of dust, which consisted of precision polymer microspheres that were levitated above a lower electrode of a radio-frequency glow-discharge plasma. Using video microscopy, they verified that the equilibrium state of this cloud of particles was a triangular lattice with a six-fold symmetry. The charge on a microsphere was $-9400\ e$ (where e is the charge of an electron), the crystalline lattice constant was 675 microns, and the mass of the 8 micron microspheres was sufficiently high that the compressional sound speed in the lattice was only 22 mm/s.

The experimenters of Ref. [13] launched two longitudinal lattice waves, with sinusoidal waveforms at different frequencies f_1 and f_2. Each of these two waves were propagating waves, and they were each excited externally by the radiation-pressure force, using laser manipulation with a steady-state laser that was amplitude modulated at the desired low frequency. The dust cloud was a horizontal monolayer. The excitation regions for the two waves were physically separate, which is a point that is important for the present paper. The spatial localization of the excitation regions was achieved by making the laser beams incident on the dust layer at an angle of 10 degrees. The experimenters then observed waves at various difference and sum frequencies, including $f_1 + f_2, f_2 - f_1, 2f_2 - f_1$, and so on. They confirmed using bi-spectral analysis that these were the products of nonlinear mixing. In this way, they provided an experimental observation of three-wave mixing, in a dusty plasma.

The physical system in that experiment can be modeled theoretically by several descriptions, including a point-like particle description and a continuum descrip-

* sanat.tiwari@iitjammu.ac.in

tion of the dust layer. The latter approach was used by Avinash *et al.* [14], who modeled the long-wavelength compressional waves in the monolayer triangular lattice, as obeying an evolution equation described by a variant of the Korteweg-de Vries (KdV) equation.

In this paper, we predict theoretically that nonlinear mixing can occur also in a different excitation configuration, where only one of the two excitation frequencies f_1 has a propagating wave that is excited locally, while the other frequency f_2 is a non-localized oscillation. In both cases, the external forcing can be provided by any physical force, including the radiation pressure force that was used in Ref. [13]. Unlike Ref. [13], only the frequency f_1 has a propagating wave that is excited in a spatially localized region, and as a crucial difference, frequency f_2 has a spatially uniform force, varying sinusoidally in time but not in space. This construction should be feasible simply by performing an experiment with a two-dimensional monolayer of dust as in the experiment of Ref. [13], but with one of the two laser beams incident on the particle cloud at zero degrees instead of ten degrees. A schematic sketch of the excitation configuration is shown in Fig. 1.

Although we are mainly concerned here with nonlinear mixing of the longitudinal lattice wave, we can mention another kind of nonlinear effect which has been observed experimentally, and that is synchronization. In synchronization, there is an inherent oscillation at one frequency and an external forcing at a second frequency. The second frequency must be close to that of the inherent oscillation, or one of its harmonics. Although synchronization has long been understood for point oscillators, it can also occur in the more complicated case of propagating waves, and indeed it is known to occur in three-dimensional dust clouds that sustain the dust acoustic wave (DAW). The DAW is self-excited at an inherent frequency due to ion flow, and an external sinusoidal forcing can be applied for example by a voltage applied to the entire cloud by an electrode so that the entire cloud experiences a global modulation [15, 16]. The result of synchronization is that the inherent oscillation is shifted in its frequency, for example to match the frequency of the external forcing. This is different from the case of mixing, where the two original waves maintain their frequencies and a third wave appears at yet another frequency. Another distinction, in comparing synchronization and mixing, is that the original two oscillations can have frequencies that differ greatly in the case of mixing, whereas for synchronization it is necessary for there to be a small difference in the two frequencies or their harmonics.

II. THEORETICAL MODEL

Our theoretical approach relies on two basic premises - (i) nonlinear compressional waves in a dusty plasma system can be modeled by a KdV equation, and (ii) the forced KdV equation can model their dynamics in the presence of an external driving force. For a three-dimensional dust cloud, the KdV equation as a model description of nonlinear DAWs is well established. It was first derived by Rao *et al.* [17] using a fluid representation of the dusty plasma and has subsequently been widely used in many theoretical and experimental studies [4, 18–20]. An fKdV model, within the fluid prescription, was first derived by Sen *et al.* [21] for describing driven nonlinear ion acoustic waves. The generic form of this model equation was subsequently shown to apply for driven DAWs as well and was successfully used to interpret the excitation of precursor dust acoustic solitons in a laboratory dusty plasma device [22, 23].

For the dust lattice wave, the KdV model has also been shown by Farokhi *et al.* [24] to theoretically describe the nonlinear evolution of waves in a two-dimensional dust lattice system. Thus one can expect the fKdV model to also successfully describe the dynamics of driven DLWs in the case of a two-dimensional lattice system subject to external forcing.

Hence as a paradigmatic model for driven compressional nonlinear oscillations in a dusty plasma system we adopt the generic fKdV equation given as,

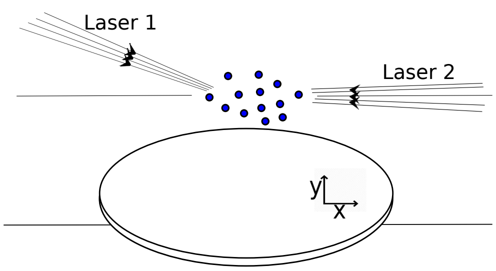

FIG. 1. A cartoon representation of a proposed experimental configuration with one of the laser beams incident on the dust at zero degrees to provide a non-localized driving oscillation. Thousands of charged dust particles, shown schematically here as a few dots, are levitated in a single horizontal layer in an electric sheath above a powered lower electrode, shown schematically as a disk at the bottom of this diagram.

$$\frac{\partial n(x,t)}{\partial t} + \alpha\, n(x,t)\frac{\partial n(x,t)}{\partial x} + \beta\frac{\partial^3 n(x,t)}{\partial x^3} = F_s(x,t) \quad (1)$$

where n is a perturbed physical quantity (representing the perturbed dust density for example) and $F_s(x,t)$ is the driving source term. The coefficients α and β represent the strengths of the nonlinear and dispersive contributions, respectively. Dissipative effects, such as may occur due to frictional damping from neutral gas particles, are not included in this model, so that it cannot describe phenomena such as synchronization that need dissipation. For $F_s(x,t) = 0$, Eq. (1) represents the standard KdV equation that has been extensively studied in the past to describe nonlinear wave propagation in neutral fluids [25], plasmas [26, 27], dusty plasmas [14, 17, 19, 28, 29] and other nonlinear dispersive media [30, 31].

The KdV equation has a variety of solutions including solitons and cnoidal wave solutions. The latter are relevant for our present work and are given by [32, 33]

$$n(x,t) = \mu\ cn^2\left[\frac{\sqrt{\mu\alpha}}{2\sqrt{\beta\kappa(\kappa+2)}}\xi(x,t);\ \kappa\right] \tag{2}$$

with

$$\xi(x,t) = \left(x - \frac{\kappa+\kappa^2-1}{\kappa(\kappa+2)}\alpha\mu t\right) \tag{3}$$

where cn is a Jacobi elliptic function. The parameter μ represents the amplitude, which can be chosen to be any value (for example, in an experiment by adjusting the amplitude of an external forcing). The elliptic parameter κ indicates the response of the medium to that amplitude. The value of the parameter κ determines the shape of the cnoidal function so that it serves as a quantitative measure of nonlinearity. For $\kappa = 0$, which is the linear case, the cnoidal solution becomes a cosine function, while for the highly nonlinear case of values close to unity, the wave form has sharp peaks and flattened bottoms. The cnoidal solution, Eq. (2), was recently shown to provide an excellent fit to experimental observations of spontaneously generated nonlinear DAWs in a three-dimensional dusty plasma cloud sustained in a RF discharge plasma [4].

The spatial wave length λ and frequency f_1 of the periodic wave, Eq. (2), are given by

$$\lambda = 4K(\kappa)\sqrt{\frac{\beta(2\kappa+\kappa^2)}{\alpha\mu}} \tag{4}$$

$$f_1 = \frac{\beta}{4K(\kappa)}(\kappa^2+\kappa-1)\left(\frac{\alpha\mu}{\beta(2\kappa+\kappa^2)}\right)^{3/2} \tag{5}$$

Here, $K(\kappa)$ is the complete elliptical integral of first kind. Expressions for the wavelength λ and frequency f_1 are obtained by comparing Eq. (2) with the following form of the solution by Dingemans *et al.* [34] and Liu *et al.* [4]

$$n(x,t) = \mu\ cn^2\left[2K(\kappa)\left(\frac{x}{\lambda} - f_1 t\right);\ \kappa\right]. \tag{6}$$

To illustrate the nature of the solution, Eq. (2), and its spectral properties we will choose $\alpha = \beta = 1$ and plot the solution for several values of κ and μ. In Fig. 2(a) we plot the time series obtained from Eq. (2) at a fixed value of x for $\mu = 0.0318$ and $\kappa = 0.001$ (such that $f_1 = 10$ Hz). The corresponding frequency spectrum is shown in Fig. 2(b). For this low value of κ, the wave form is approximately sinusoidal and shows a single dominant frequency $f_1 = 10$ Hz in the spectrum. A small peak at $2f_1$ due to the nonzero nonlinearity ($\kappa \neq 0$) is also observed. For a higher value of $\kappa = 0.8$ and $\mu = 78$ (such that f_1 is still 10 Hz) the wave form is more nonlinear in character, as shown in Fig. 2(c), and the spectrum Fig. 2(d) shows the appearance of higher harmonics at $2f_1$, $3f_1$ *etc.*

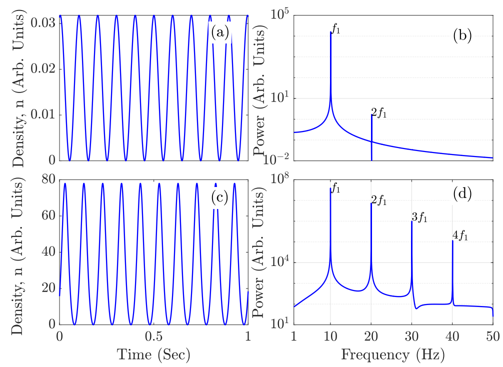

FIG. 2. Time series and the corresponding power spectra for an arbitrary spontaneous density perturbation, n, as given by Eq. (2). (a) Sinusoidal-like wave with $\kappa = 0.001$, $\mu = 0.0318$ such that $f_1 = 10$ Hz. (b) Power spectrum of (a). (c) Nonlinear wave form with $\kappa = 0.8$, $\mu = 78$ and $f_1 = 10$ Hz. (d) Power spectrum of (c).

III. EXACT NONLINEAR SOLUTION AND NONLINEAR WAVE MIXING

We next examine the solution of the fKdV model equation, Eq. (1), with a specific form of the driving term. For a sinusoidally time varying driver, $F_s(x,t) = A_s\sin(2\pi f_2 t)$, Eq. (1) has an exact analytic solution (derived using Hirota's method as in Salas *et al.* [35]) given by

$$\begin{aligned} n(x,t) &= -\frac{A_s\cos(2\pi f_2 t)}{2\pi f_2} + \mu\ cn^2\left[\frac{\sqrt{\mu\alpha}}{2\sqrt{\beta\kappa(\kappa+2)}}\eta(x,t);\ \kappa\right] \\ \eta(x,t) &= \left(x - \frac{\kappa+\kappa^2-1}{\kappa(\kappa+2)}\alpha\mu t + \frac{A_s\alpha}{(2\pi f_2)^2}\sin(2\pi f_2 t)\right). \end{aligned} \tag{7}$$

To explore the phenomenon of wave mixing in various nonlinear regimes, we will use this exact solution for different values of the parameters, κ and μ. Now that we are driving not only at frequency f_1, but also at frequency f_2, we see a modulation in the time series of Fig. 3(a) and 3(c), obtained from Eq. (7). The corresponding spectra are shown in Fig. 3(b) and 3(d), respectively. The conditions are for a weakly nonlinear amplitude in Fig. 3(a) and 3(c), with $\mu = 0.0318$, $\kappa = 0.001$ and $A_s = 0.318$. The amplitude is greater and more nonlinear in Fig. 3(b) and 3(d), with $\mu = 78$, $\kappa = 0.8$ and $A_s = 780$. In all cases

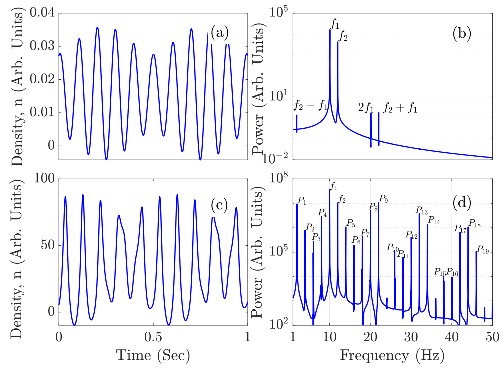

FIG. 3. Time series and the corresponding power spectra for a density perturbation, n, driven at $f_2 = 12$ Hz from Eq. (7). (a) Time series with weak nonlinearity ($\kappa = 0.001$, $\mu = 0.0318$, $f_1 = 10$ Hz, $A_s = 0.318$) and (b) the corresponding power spectra showing f_1, f_2 and their sum and difference frequencies. (c) Time series with large nonlinearity ($\kappa = 0.8$, $\mu = 78$, $f_1 = 10$ Hz, $A_s = 780$) and (d) its corresponding power spectra showing f_1, f_2, their sum and difference frequencies and their harmonics.

for Fig. 3, $f_1 = 10$ Hz, $f_2 = 12$ Hz, and $\alpha = \beta = 1$. The spectrum shows peaks at f_1, f_2, sum-frequency $f_2 + f_1$ and difference-frequency $f_2 - f_1$.

Nonlinear mixing is revealed by the presence of combination frequencies in the spectra of Fig. 3. Especially in Fig. 3(d) with the higher amplitude and greater nonlinearity, we see many combination frequencies such as $2f_2 - f_1$ which is labeled as peak P_5, and $2f_1 + f_2$ which is labeled as peak P_{13}. There is a rich variety of these combination frequencies, and they are listed in Table I. The presence of peaks at harmonics such as $2f_1$, $3f_1$ and $4f_1$ are not attributed to mixing, but rather just the presence of nonlinearity ($\kappa > 0$) in the excitation.

TABLE I. Dominant frequencies observed in the spectral data shown in Fig. 3(d).

f_1	10	f_2	12
P_1	$f_2 - f_1$	P_{11}	$4f_2 - 2f_1$
P_2	$2(f_2 - f_1)$	P_{12}	$3f_1$
P_3	$3(f_2 - f_1)$	P_{13}	$2f_1 + f_2$
P_4	$4(f_2 - f_1)$	P_{14}	$2f_2 + f_1$
P_5	$2f_2 - f_1$	P_{15}	$4f_2 - f_1$
P_6	$3f_2 - 2f_1$	P_{16}	$4f_1$
P_7	$4f_2 - 3f_1$	P_{17}	$3f_1 + f_2$
P_8	$2f_1$	P_{18}	$2(f_1 + f_2)$
P_9	$f_2 + f_1$	P_{19}	$f_1 + 3f_2$
P_{10}	$3f_2 - f_1$		

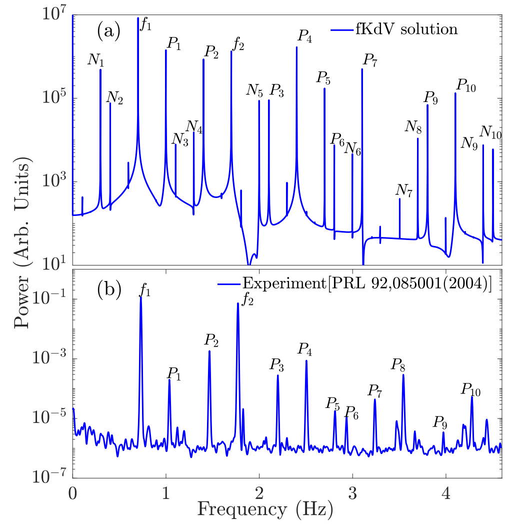

FIG. 4. Comparison of time series power spectra for [a] obtained from the fKdV model, Eq. (7), and [b] we have replotted the same experimental data points that were originally reported in Ref. [13]. Parameters used for the theoretical model are $\mu = 18.5, \kappa = 0.7$ (corresponds to $f_1 = 0.7$ Hz), $A_s = 18.5$ and $f_2 = 1.7$ Hz.

IV. DISCUSSION

As a specimen to illustrate a spectrum that is known to exhibit nonlinear mixing, we have replotted in Fig. 4(b) the experimental spectrum from Ref. [13]. This experimental spectrum includes peaks at combination frequencies such as $2f_2 - f_1$ and $2f_1 + f_2$. (The experiment also has peaks at harmonics such as $2f_1$ and $3f_1$, but those can occur in the absence of mixing due to the non-sinusoidal distortion of a periodic waveform, as is common under nonlinear effects.)

It is significant that the spectrum from our solution of the fKdV equation shows peaks at the same combination frequencies as for the experiment of Ref. [13]. This observation gives us some confidence that we are observing nonlinear mixing. The model, even though it is simple, adequately captures salient mechanisms for nonlinear mixing, yielding the same signatures of combination frequencies as in a specimen experimental system.

Although for Fig. 4(a) we used the same excitation frequencies $f_1 = 0.7$ Hz and $f_2 = 1.7$ Hz as for the experiment of Ref. [13], we should mention several ways that the model's assumptions differ from that of experiment. First, there is frictional damping from gas in the experiment. This friction can inhibit nonlinear effects, unless a threshold is exceeded, which would not be the case in the model where there was no friction. Second,

TABLE II. Frequencies observed in Fig. 4.

Frequency (Hz)	Fig. 4(a)	Fig. 4(b)
f_1	0.7	0.7
f_2	1.7	1.7
$P_1 = f_2 - f_1$	✓	✓
$P_2 = 2f_1$	✓	✓
$P_3 = 3f_1$	✓	✓
$P_4 = f_1 + f_2$	✓	✓
$P_5 = 2f_2 - f_1$	✓	✓
$P_6 = 4f_1$	✓	✓
$P_7 = 2f_1 + f_2$	✓	✓
$P_8 = 2f_2$		✓
$P_9 = 3f_1 + f_2$	✓	✓
$P_{10} = 2f_2 + f_1$	✓	✓
$N_1 = f_2 - 2f_1$	✓	
$N_2 = 3f_1 - f_2$	✓	
$N_3 = 4f_1 - f_2$	✓	
$N_4 = 2f_2 - 3f_1$	✓	
$N_5 = 2(f_2 - f_1)$	✓	
$N_6 = 3(f_2 - f_1)$	✓	
$N_7 = 5f_1$	✓	
$N_8 = 3f_2 - 2f_1$	✓	
$N_9 = 3f_2 - f_1$	✓	
$N_{10} = 4f_1 + f_2$	✓	

the experimental system was finite in size and could exhibit an overall sloshing mode oscillation in the presence of the external confining potential, which is provided by a curved sheath above the horizontal electrode. Thus, the experimental spectrum could potentially include the signature of a sloshing mode oscillation, or the mixing of that oscillation with the excitation at f_1 or f_2. This behavior would not be described by our model. Third, the model was constructed so that it assumes that the excitation at one of the two frequencies is not a propagating wave, but is uniformly applied throughout the medium, as sketched in Fig. 1. This third difference might be less substantial than one might expect, however, because the wavelength at the low frequency $f_1 = 0.7$ Hz in the experiment could have been substantial as compared to the finite size of the cloud of charged dust particles.

We also note that the spectral peaks obtained from the theoretical fKdV model in Fig. 4(a) are not limited to all those present in the experimental spectrum shown in Fig. 4(b). In Table II, we list those peaks P_1-P_{10} of the theoretical model that are also present in the experimental spectrum while peaks N_1-N_{10} are only present in the theoretical model. The latter frequency peaks represent different combinations of the sum and difference of f_1, f_2 and their higher harmonics. Their absence in the experimental spectrum could be due to the effect of gas friction, which can prevent weak nonlinear effects from being observed.

V. CONCLUSIONS

To conclude, we have presented a simple mathematical model consisting of a forced KdV equation with a time varying sinusoidal forcing term that shows the existence of nonlinear wave mixing in a dusty plasma medium. Physically the model represents wave mixing arising from the temporal modulation of a nonlinear dust compressional wave. This is a situation that can be easily realized in an experiment using radiation pressure of lasers or time varying electric potentials to modulate self-excited or externally driven large amplitude compressional waves.

One advantage of the present model is the existence of an exact analytic solution which can be conveniently used to map various parametric regimes without recourse to a numerical solution of the nonlinear equation. This solution not only shows the existence of wave mixing phenomenon in this simple model system but may also be useful in predicting nonlinear wave mixing for a proposed experimental configuration in a two-dimensional dusty plasma medium.

ACKNOWLEDGMENTS

Work done by ST and AM was supported by IIT Jammu seed grant No. SG0012. JG acknowledges NASA-JPL subcontract No. 1573629 and U.S. DOE grant DE-SC0014566. CC and GG acknowledge NASA-JPL subcontract No. 1573108 and NRL Base Funds. AS is thankful to the Indian National Science Academy (INSA) for their support under the INSA Senior Scientist Fellowship scheme.

DATA AVAILABILITY

Data sharing is not applicable to this article as no new data were created or analyzed in this study.

[1] K. O. Hill, D. C. Johnson, B. S. Kawasaki, and R. I. MacDonald, J. Appl. Phys. **49**, 5098 (1978).
[2] P. Fischer, D. S. Wiersma, R. Righini, B. Champagne, and A. D. Buckingham, Phys. Rev. Lett. **85**, 4253 (2000).
[3] Y. Shi, Phys. Rev. E **99**, 063212 (2019).
[4] B. Liu, J. Goree, T. M. Flanagan, A. Sen, S. K. Tiwari, G. Ganguli, and C. Crabtree, Phys. Plasmas **25**, 113701 (2018).
[5] L.-W. Teng, M.-C. Chang, Y.-P. Tseng, and L. I, Phys. Rev. Lett. **103**, 245005 (2009).

[6] A. Homann, A. Melzer, S. Peters, and A. Piel, Phys. Rev. E **56**, 7138 (1997).
[7] F. Melandsø, Phys. Plasmas **3**, 3890 (1996).
[8] A. Barkan, R. L. Merlino, and N. D'Angelo, Phys. Plasmas **2**, 3563 (1995).
[9] J. Heinrich, S.-H. Kim, and R. L. Merlino, Phys. Rev. Lett. **103**, 115002 (2009).
[10] T. Deka, A. Boruah, S. K. Sharma, and H. Bailung, Phys. Plasmas **24**, 093706 (2017).
[11] S. Nunomura, D. Samsonov, and J. Goree, Phys. Rev. Lett. **84**, 5141 (2000).
[12] A. Homann, A. Melzer, S. Peters, R. Madani, and A. Piel, Phys. Lett. A **242**, 173 (1998).
[13] V. Nosenko, K. Avinash, J. Goree, and B. Liu, Phys. Rev. Lett. **92**, 085001 (2004).
[14] K. Avinash, P. Zhu, V. Nosenko, and J. Goree, Phys. Rev. E **68**, 046402 (2003).
[15] W. D. S. Ruhunusiri and J. Goree, Phys. Rev. E **85**, 046401 (2012).
[16] T. Deka, B. Chutia, Y. Bailung, S. K. Sharma, and H. Bailung, Plasma Sci. Technol. **22**, 045002 (2020).
[17] N. N. Rao, P. K. Shukla, and M. Y. Yu, Planet. Space Sci. **38**, 543 (1990).
[18] P. K. Shukla and A. A. Mamun, New J. Phys. **5**, 17 (2003).
[19] P. Bandyopadhyay, G. Prasad, A. Sen, and P. K. Kaw, Phys. Rev. Lett. **101**, 065006 (2008).
[20] P. Bandyopadhyay, U. Konopka, S. A. Khrapak, G. E. Morfill, and A. Sen, New J. Phys. **12**, 073002 (2010).
[21] A. Sen, S. Tiwari, S. Mishra, and P. Kaw, Adv. Space Res. **56**, 429 (2015).
[22] S. Jaiswal, P. Bandyopadhyay, and A. Sen, Phys. Rev. E **93**, 041201 (2016).
[23] G. Arora, P. Bandyopadhyay, M. G. Hariprasad, and A. Sen, Phys. Plasmas **26**, 093701 (2019).
[24] B. Farokhi, P. Shukla, N. Tsintsadze, and D. Tskhakaya, Phys. Lett. A **264**, 318 (1999).
[25] G. M. Peradze and N. L. Tsintsadze, Low Temp. Phys. **45**, 103 (2019).
[26] D. A. Fogaça, F. S. Navarra, and L. G. Ferreira Filho, Phys. Rev. D **84**, 054011 (2011).
[27] Y. C. Mo, R. A. Kishek, D. Feldman, I. Haber, B. Beaudoin, P. G. O'Shea, and J. C. T. Thangaraj, Phys. Rev. Lett. **110**, 084802 (2013).
[28] D. Samsonov, A. V. Ivlev, R. A. Quinn, G. Morfill, and S. Zhdanov, Phys. Rev. Lett. **88**, 095004 (2002).
[29] S. K. Sharma, A. Boruah, and H. Bailung, Phys. Rev. E **89**, 013110 (2014).
[30] H. Leblond, Phys. Rev. A **78**, 013807 (2008).
[31] A. Gasch, T. Berning, and D. Jäger, Phys. Rev. A **34**, 4528 (1986).
[32] E. F. El-Shamy, Phys. Rev. E **91**, 033105 (2015).
[33] A. R. Osborne, Phys. Rev. E **48**, 296 (1993).
[34] M. Dingemans, *Water Wave Propagation Over Uneven Bottoms*, Advanced Series on Ocean Engineering (World Scientific, Singapore, 1997).
[35] A. H. Salas, Nonlinear Anal. Real World Appl. **12**, 1314 (2011).

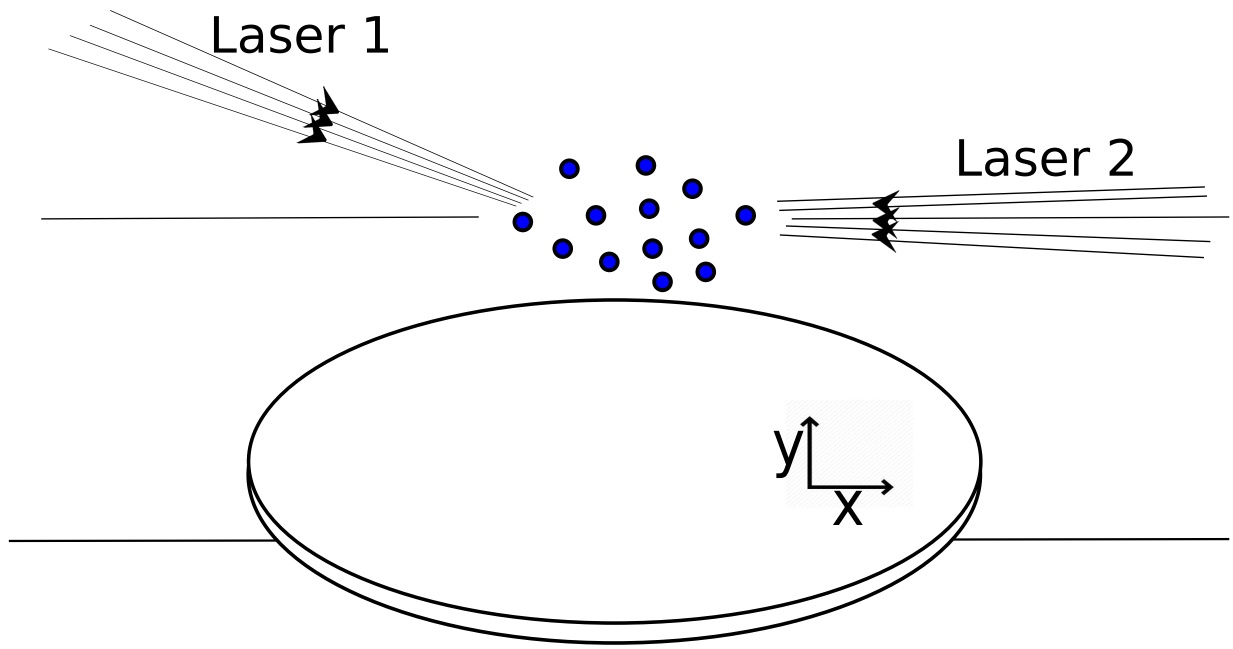
Laser 1
Laser 2
y
x

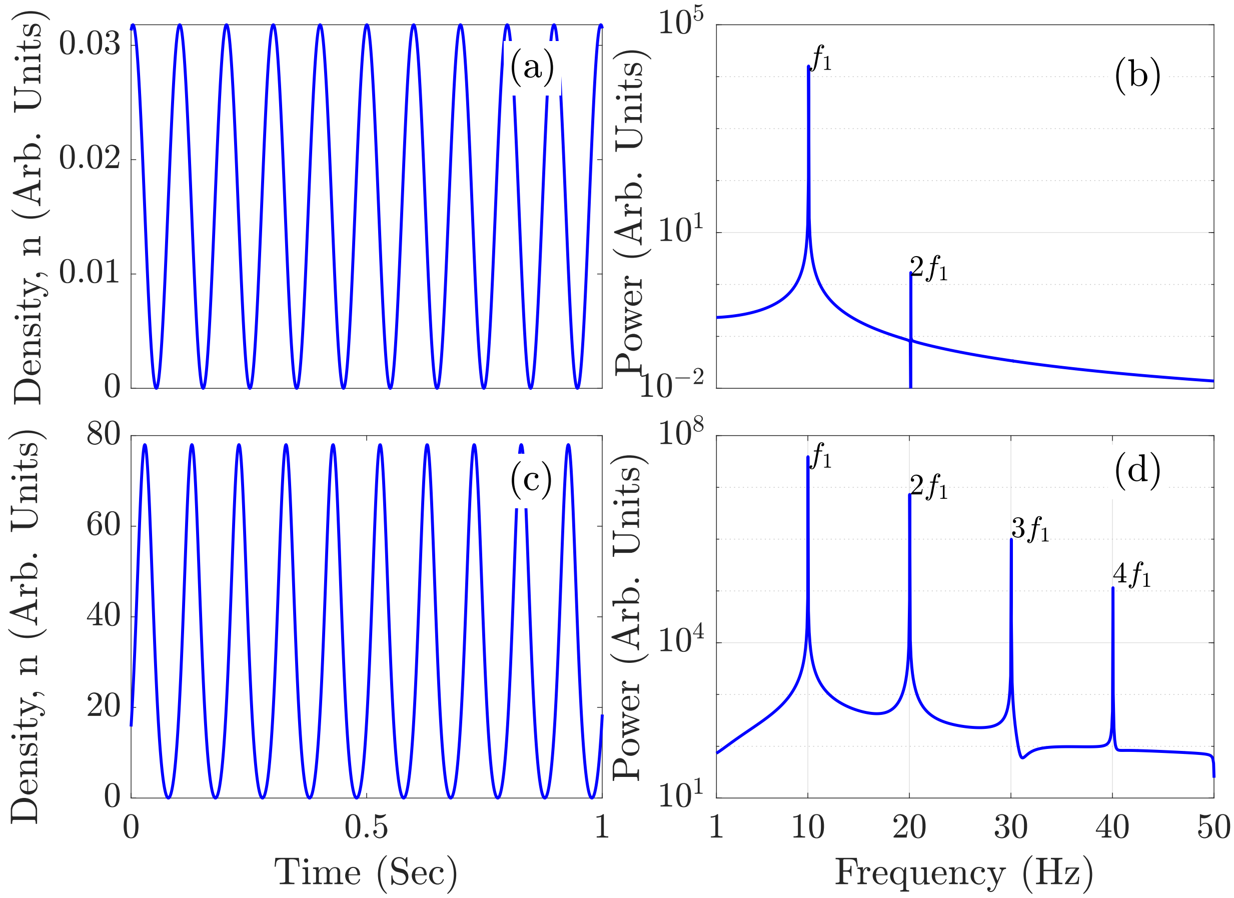
(a)
(b)
(c)
(d)
Density, n (Arb. Units)
Power (Arb. Units)
Time (Sec)
Frequency (Hz)
f_1
$2f_1$
$3f_1$
$4f_1$
0.03
0.02
0.01
0
80
60
40
20
0.5
1
10^5
10^1
10^{-2}
10^8
10^4
10^1
10
30
50

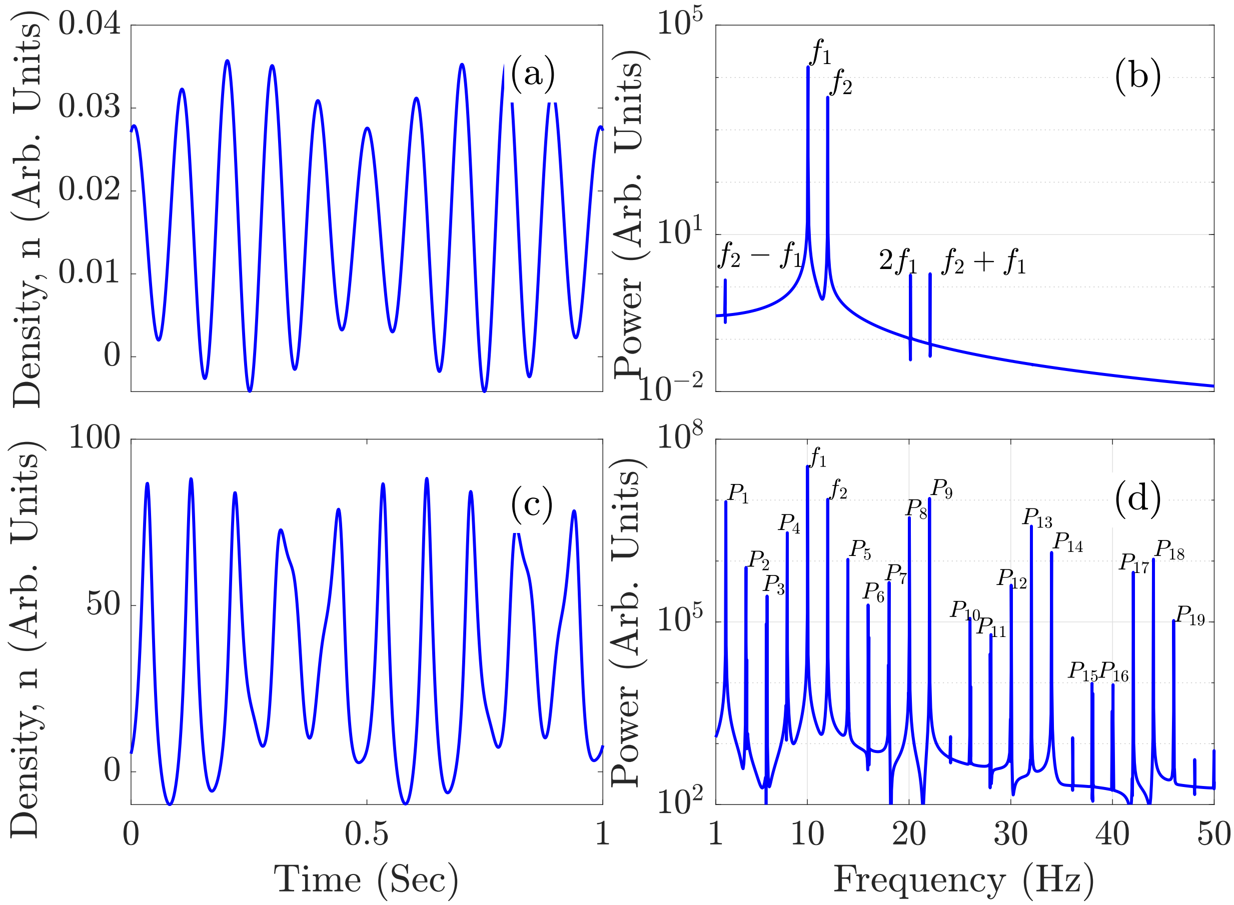
(a)
(b)
(c)
(d)
Density, n (Arb. Units)
Power (Arb. Units)
Time (Sec)
Frequency (Hz)
f_1
f_2
$f_2 - f_1$
$2f_1$
$f_2 + f_1$
P_1 P_2 P_3 P_4 P_5 P_6 P_7 P_8 P_9 P_{10} P_{11} P_{12} P_{13} P_{14} P_{15} P_{16} P_{17} P_{18} P_{19}

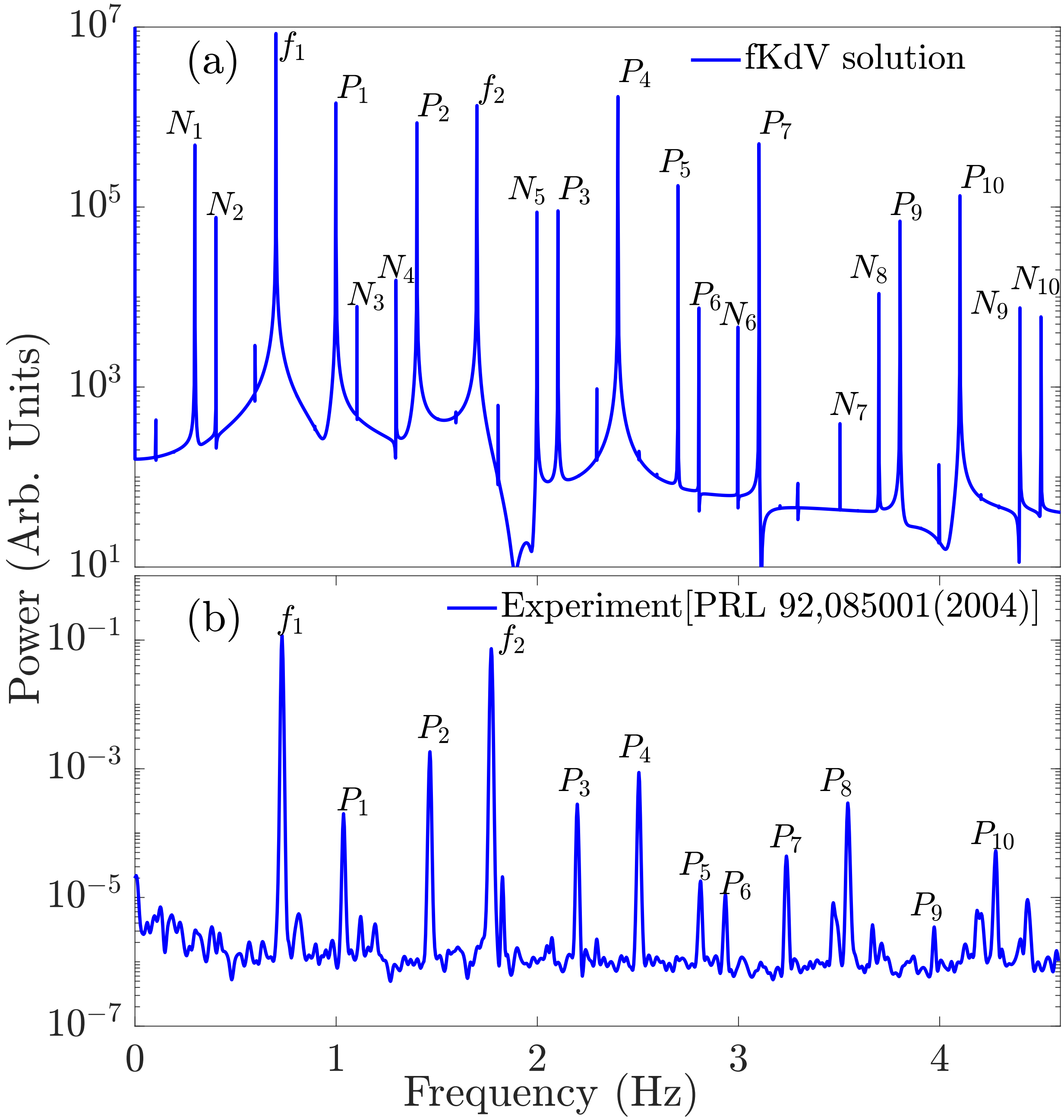
(a)
fKdV solution
(b)
Experiment[PRL 92,085001(2004)]
Power (Arb. Units)
Frequency (Hz)
f_1
f_2
N_1
N_2
N_3
N_4
N_5
N_6
N_7
N_8
N_9
N_{10}
P_1
P_2
P_3
P_4
P_5
P_6
P_7
P_8
P_9
P_{10}
10^7
10^5
10^3
10^1
10^{-1}
10^{-3}
10^{-5}
10^{-7}
0
1
2
3
4